LETTER

Non–invasive imaging through opaque scattering layers

Jacopo Bertolotti[1,2]*, Elbert G. van Putten[1]†*, Christian Blum[3], Ad Lagendijk[1,4], Willem L. Vos[1] & Allard P. Mosk[1]

Non-invasive optical imaging techniques, such as optical coherence tomography[1–3], are essential diagnostic tools in many disciplines, from the life sciences to nanotechnology. However, present methods are not able to image through opaque layers that scatter all the incident light[4,5]. Even a very thin layer of a scattering material can appear opaque and hide any objects behind it[6]. Although great progress has been made recently with methods such as ghost imaging[7,8] and wavefront shaping[9–11], present procedures are still invasive because they require either a detector[12] or a nonlinear material[13] to be placed behind the scattering layer. Here we report an optical method that allows non-invasive imaging of a fluorescent object that is completely hidden behind an opaque scattering layer. We illuminate the object with laser light that has passed through the scattering layer. We scan the angle of incidence of the laser beam and detect the total fluorescence of the object from the front. From the detected signal, we obtain the image of the hidden object using an iterative algorithm[14,15]. As a proof of concept, we retrieve a detailed image of a fluorescent object, comparable in size (50 micrometres) to a typical human cell, hidden 6 millimetres behind an opaque optical diffuser, and an image of a complex biological sample enclosed between two opaque screens. This approach to non-invasive imaging through strongly scattering media can be generalized to other contrast mechanisms and geometries.

As experienced on a foggy day, scattering of light severely impairs our ability to see. A strongly scattering medium allows light to pass in the form of a diffuse halo, but completely scrambles all the spatial information[6]. A strategy that has proved very successful in imaging through scattering materials is to separate the small amount of light that did not change direction owing to random scattering (ballistic light) from the scattered background using a gated technique such as optical coherence tomography[1–3]. In this way it is possible to obtain sharp images through semi-transparent media, but for stronger scattering the medium appears opaque to the eye and prevents present non-invasive optical imaging techniques from obtaining detailed images[5]. Absorptive objects deep inside a scattering medium can be located using diffuse wave tomography, which does not allow one to resolve details much smaller than the depth[16,17].

Speckle correlations can be used to transmit highly detailed image information through scattering media[9,18–21]. To demonstrate non-invasive imaging with speckle correlations, we constructed the set-up illustrated in Fig. 1a. A 50-µm-wide fluorescent object made of dye-doped polymer (Supplementary Information) is placed a distance $d = 6$ mm behind a scattering layer (an Edmund Optics 120-grit ground-glass diffuser) that completely hides it. As shown in Fig. 1b, the scattering layer makes it impossible to resolve even millimetre-sized details at this distance. We shine a laser (wavelength, 532 nm) on the scattering layer where, owing to the scattering, the transmitted light produces a speckle pattern that illuminates the object. The fluorescent

light is scrambled by scattering and through the diffuser we cannot measure any spatial information about the shape of the object (Fig. 1c). However, the total amount of transmitted fluorescence can be measured and retains the information on the overlap between the object's fluorescent response, $O(r)$, and the speckle intensity, $S(r)$, where r is the vector of spatial coordinates.

In our measurement procedure, we scan the angle of incidence, $\theta = (\theta_x, \theta_y)$, of the laser beam using a pair of scanning galvanic mirrors (Supplementary Information). Although the speckle illuminating the object might appear random, it contains correlations that can be exploited. In particular, the angular correlation known as the memory effect[22,23] means that rotating the incident beam over small angles θ does not change the resulting speckle pattern but only translates it over a distance $\Delta r \approx \theta d$. Therefore, up to a proportionality constant that we will set to 1, the total measured fluorescence as a function of the incident angle is given by
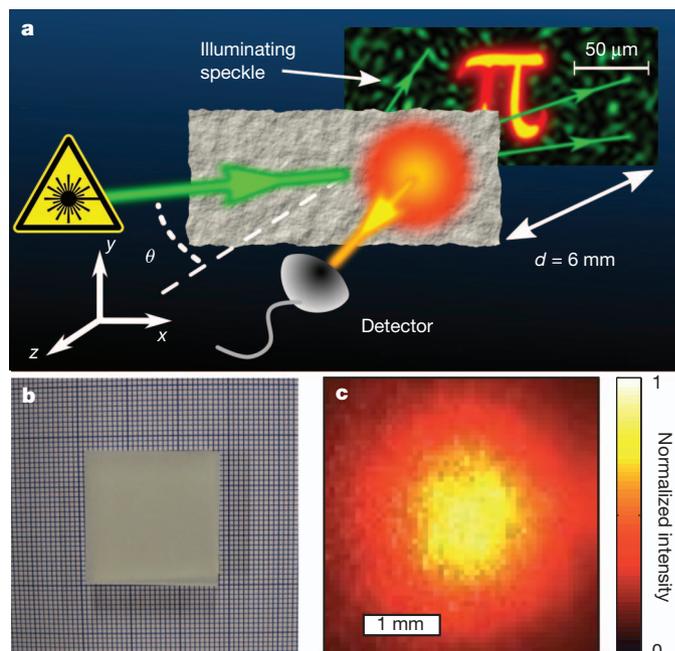

Figure 1 | Schematic of the apparatus for non-invasive imaging through strongly scattering layers. a, A monochromatic laser beam illuminates an opaque layer of thickness L at an angle θ. A fluorescent object is hidden a distance $d = 6$ mm behind the layer. The fluorescent light is detected from the front of the scattering layer by a charge-coupled device camera. **b**, Photograph of the scattering layer a distance $d = 6$ mm from a millimetre-grid background. The grid behind the layer is completely hidden. **c**, Intensity of fluorescence emitted by the hidden object, as measured in front of the scattering layer. A single fluorescent image contains no information on the shape of the object.

[1]Complex Photonic Systems (COPS), MESA+ Institute for Nanotechnology, University of Twente, PO Box 217, 7500 AE Enschede, The Netherlands. [2]University of Florence, Dipartimento di Fisica, 50019 Sesto Fiorentino, Italy. [3]Nanobiophysics (NBP), MESA + Institute for Nanotechnology, University of Twente, PO Box 217, 7500 AE Enschede, The Netherlands. [4]FOM Institute for Atomic and Molecular Physics, Science Park 104, 1098 XG Amsterdam, The Netherlands. †Present address: Philips Research Laboratories, 5656 AE Eindhoven, The Netherlands.
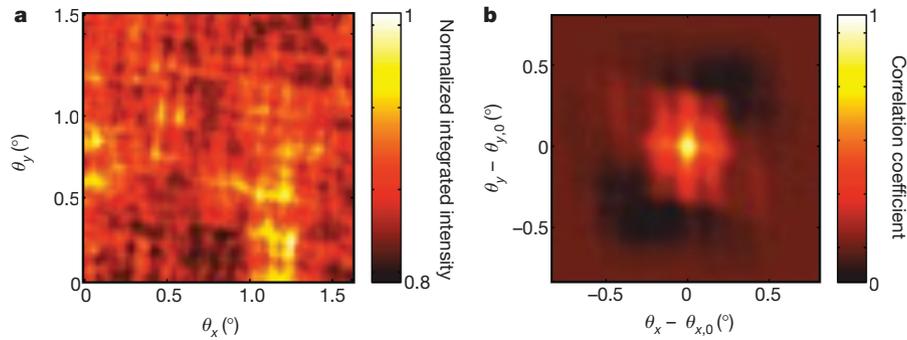*These authors contributed equally to this work.

Figure 2 | Experimental retrieval of the hidden object's autocorrelation.
a, Integrated fluorescent intensity, I, as a function of the incident angle, $\theta = (\theta_x, \theta_y)$. **b**, Autocorrelation $I \star I$ averaged over nine scans taken at different values of the starting incidence angle, θ_0, to average over the different realizations of the speckle, S.

$$I(\theta) = \int_{-\infty}^{\infty} O(r)S(r - \theta d)\, \mathrm{d}^2 r = [O * S](\theta)$$

where $*$ denotes the convolution product. Owing to the random nature of the speckle pattern, the measured intensity, $I(\theta)$ (Fig. 2a), does not directly resemble that of the original hidden object. Instead, the image information is encoded in the correlations of the measured signal.

To separate the shape of the object from the random speckle, we calculate the autocorrelation product of the measured intensity and obtain

$$\langle I \star I \rangle (\Delta\theta) = \langle O * S \rangle \star \langle O * S \rangle$$
$$= \langle O \star O \rangle * \langle S \star S \rangle = [O \star O] * \langle S \star S \rangle$$

where $\star$ is the cross-correlation product and angle brackets denote the average over speckle realizations (that is, the average over different scans). Because the average autocorrelation of a speckle pattern, $\langle S \star S \rangle$, is a sharply peaked function[24], we are effectively measuring the auto-correlation of the object $O \star O$ with a resolution given by the average speckle size. For a circular illumination beam of width W, we find that

$$\langle I \star I \rangle (\Delta\theta) = \left[[O \star O] * \left(\frac{2J_1(k|\theta|W)}{k|\theta|W} \right)^2 \right](\Delta\theta) \times \left(\frac{k|\Delta\theta|L}{\sinh(k|\Delta\theta|L)} \right)^2 \tag{1}$$

where J_1 is a first-order Bessel function of the first kind, L is the layer thickness and k is the wavenumber[24]. The second term in the convolution represents the average speckle size and can be made arbitrarily close to the diffraction limit by increasing W. The final (multiplicative) factor accounts for the fact that when the change in the angle of incidence of the laser is not small enough the speckle pattern is not only rotated but also decorrelates, effectively limiting the memory range[22–25] and, thus, the available field of view. We note that ground-glass diffusers are effectively single scattering layers and thus have a very large memory range while being completely opaque[25] (Supplementary Information). Equation (1) does not depend on the detailed scattering properties of the scattering layer, allowing us to measure $O \star O$ for objects hidden behind any completely opaque layer.

The average autocorrelation of nine subsequent scans is shown in Fig. 2b. We obtained the independent measurements of $I(\theta)$ needed to average $S \star S$ by starting each scan at a different incidence angle. In fact, if the difference between the starting angles is larger than the angular size of the object, the speckle realizations are independent. Comparing the measured autocorrelation with a microscope image of the object (Fig. 3a), we recognize some features such as the presence of two vertical legs. Yet an autocorrelation contains only information on the relative distance between the various parts of an object, and not directly on the object itself. Furthermore, the autocorrelation of a real

object is always centred and centrosymmetric. To obtain an image of the object we need to invert the autocorrelation.

In two and three dimensions, autocorrelations can be numerically inverted using a Gerchberg–Saxton-type iterative algorithm by exploiting some manifest properties of the measured signal as constraints[14,26]. In our case, we used the fact that a fluorescent image is always real and positive. Other common choices are the fact that O is a real function, as in stellar speckle interferometry[27], and the positiveness of both the real and the imaginary part of O, as in X-ray scattering[15,28]. We used a standard version of this algorithm, which can perform the inversion in a few seconds on a normal desktop computer (Supplementary Information). The results of the inversion are shown in Fig. 3. In Fig. 3a we show a fluorescence microscope image of the object before it is placed behind the scattering layer, and in Fig. 3b we show the object retrieved from the measured autocorrelation presented in Fig. 2b. The two images of the symbol π show an excellent resemblance to each other. Small features such as the flattening of the left 'foot' of the symbol or the inhomogeneities in the intensity are faithfully recovered, demonstrating successful imaging of the object through an opaque layer.

To test our method on a complex biological sample, we placed a slice of the stem of *Convallaria majalis* between two diffusers (4.5 cm behind the front one and 6 mm in front of the back one), effectively enclosing the sample. The structure presents intracellular autofluorescence and did not require staining. The light emitted when the sample was illuminated with the speckled light was collected from behind the back diffuser (Fig. 4a), and after averaging over five scans we obtained the autocorrelation shown in Fig. 4b. Figures 4c and 4d respectively show an image of the sample taken with the back diffuser removed (thus allowing free optical access) and the reconstructed image obtained starting from the measured autocorrelation. The blue lines in Fig. 4c are contours of the reconstructed image at 20% of the maximum intensity, showing that all the high-intensity features of the
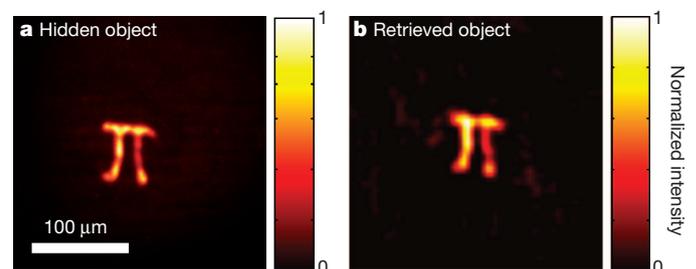

Figure 3 | Comparison of the retrieved image with the hidden object.
a, Fluorescence microscope image of the object taken without the scattering layer in place. **b**, The retrieved object that we found from the measured autocorrelation in Fig. 2b. Even small details such as the intensity inhomogeneities of the original object are recovered in the retrieved image.
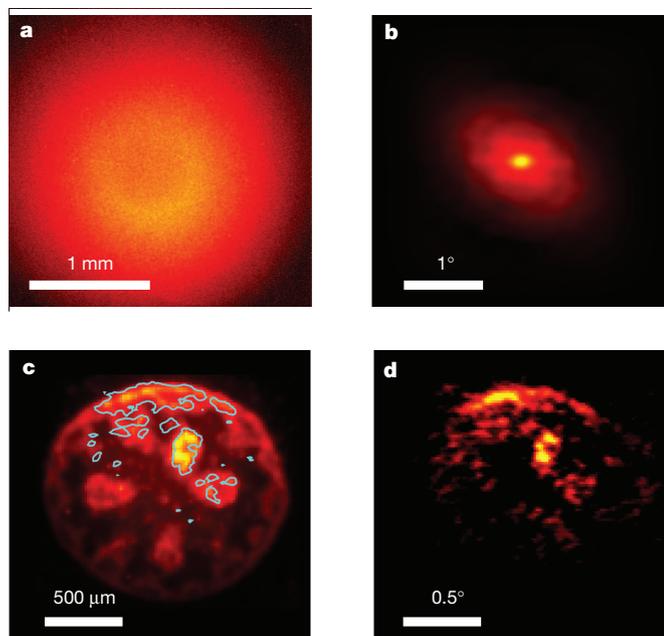
Figure 4 | Retrieval of a complex, biological structure. a, Autofluorescence from the sample of *C. majalis* as seen through the back diffuser. **b**, Measured autocorrelation averaged over five scans. **c**, Fluorescence image of the structure taken after removing the back diffuser and averaging over many (~200) speckle illuminations. The blue line is a contour (at 20% of the maximum intensity) of the reconstructed object. **d**, The reconstructed object. All high-intensity features in the original object are recovered. The colour scale is the same as in Fig. 3.

object were faithfully recovered. To reduce the complexity of the reconstruction, we lowered the resolution by increasing the speckle size. Higher resolution (up to the diffraction limit) can be obtained by decreasing the size of the speckle spots. The main limitation on the reconstruction fidelity is given by the background signal, which can distort the measured autocorrelation[29].

We have experimentally demonstrated non-invasive imaging of a two-dimensional fluorescent object through a completely opaque layer. Other optical signals that depend on speckle intensity, such as chemically selective Raman scattering, photoacoustic absorption contrast[30] and second-harmonic generation, can also be used. Three-dimensional imaging, for example to study cell morphology[4], is possible by also scanning the speckle pattern in the third direction, which can be done by adding a parabolic phase pattern to the beam.

METHODS SUMMARY

A collimated laser beam was shone on the scattering layer with a controllable angle of incidence. The total amount of fluorescent light coming from the hidden object was detected through the scattering layer as a function of the angle of incidence, using a charge-coupled device. After subtracting the background, the measured signal was autocorrelated and the autocorrelations obtained from several independent scans were averaged. The resulting average autocorrelation was multiplied with a Hamming window and used as the input for a Gerchberg–Saxton-type iterative algorithm that can be used to determine the shape of the hidden object.

1. Abramson, N. Light-in-flight recording by holography. *Opt. Lett.* **3,** 121–123 (1978).
2. Huang, D. *et al.* Optical coherence tomography. *Science* **254,** 1178–1181 (1991).
3. Nasr, M. B., Saleh, B. E. A., Sergienko, A. V. & Teich, M. C. Demonstration of dispersion-canceled quantum-optical coherence tomography. *Phys. Rev. Lett.* **91,** 083601 (2003).
4. Ntziachristos, V. Going deeper than microscopy: the optical imaging frontier in biology. *Nature Methods* **7,** 603–614 (2010).
5. Ishimaru, A., Sermsak, J. & Kuga, Y. Imaging through random multiple scattering media using integration of propagation and array signal processing. *Waves Rand. Compl. Media* **22,** 24–39 (2012).
6. Sheng, P. *Introduction to Wave Scattering, Localization and Mesoscopic Phenomena* (Academic, 1995).
7. Strekalov, D. V., Sergienko, A. V., Klyshko, D. N. & Shih, Y. H. Observation of two-photon "ghost" interference and diffraction. *Phys. Rev. Lett.* **74,** 3600–3603 (1995).
8. Bennink, R. S., Bentley, S. J. & Boyd, R. W. "Two-photon" coincidence imaging with a classical source. *Phys. Rev. Lett.* **89,** 113601 (2002).
9. Freund, I. Looking through walls and around corners. *Physica A* **168,** 49–65 (1990).
10. Mosk, A. P., Lagendijk, A., Lerosey, G. & Fink, M. Controlling waves in space and time for imaging and focusing in complex media. *Nature Photon.* **6,** 283–292 (2012).
11. Katz, O., Small, E. & Silberberg, Y. Focusing and compression of ultrashort pulses through scattering media. *Nature Photon.* **5,** 372–377 (2011).
12. van Putten, E. G. *et al.* Scattering lens resolves sub-100 nm structures with visible light. *Phys. Rev. Lett.* **106,** 193905 (2011).
13. Hsieh, C.-L., Pu, Y., Grange, R., Laporte, G. & Psaltis, D. Imaging through turbid layers by scanning the phase conjugated second harmonic radiation from a nanoparticle. *Opt. Express* **18,** 20723–20731 (2010).
14. Fienup, J. R. Phase retrieval algorithms: a comparison. *Appl. Opt.* **21,** 2758–2769 (1982).
15. Miao, J., Charalambous, P., Kirz, J. & Sayre, D. Extending the methodology of X-ray crystallography to allow imaging of micrometre-sized non-crystalline specimens. *Nature* **400,** 342–344 (1999).
16. Gibson, A., Hebden, J. & Arridge, S. Recent advances in diffuse optical imaging. *Phys. Med. Biol.* **50,** R1–R43 (2005).
17. Culver, J. P., Ntziachristos, V., Holboke, M. J. & Yodh, A. G. Optimization of optode arrangements for diffuse optical tomography: a singular-value analysis. *Opt. Lett.* **26,** 701–703 (2001).
18. Fink, M. Time reversed acoustics. *Phys. Today* **50,** 34–40 (1997).
19. Yaqoob, Z., Psaltis, D., Feld, M. S. & Yang, C. Optical phase conjugation for turbidity suppression in biological samples. *Nature Photon.* **2,** 110–115 (2008).
20. Popoff, S. M. *et al.* Measuring the transmission matrix in optics: an approach to the study and control of light propagation in disordered media. *Phys. Rev. Lett.* **104,** 100601 (2010).
21. Vellekoop, I. M. & Aegerter, C. Scattered light fluorescence microscopy: imaging through turbid layers. *Opt. Lett.* **35,** 1245–1247 (2010).
22. Feng, S., Kane, C., Lee, P. A. & Stone, A. D. Correlations and fluctuations of coherent wave transmission through disordered media. *Phys. Rev. Lett.* **61,** 834–837 (1988).
23. Freund, I., Rosenbluh, M. & Feng, S. Memory effects in propagation of optical waves through disordered media. *Phys. Rev. Lett.* **61,** 2328–2331 (1988).
24. Akkermans, E. & Montambaux, G. *Mesoscopic Physics of Electrons and Photons* 427–439 (Cambridge Univ. Press, 2007).
25. Katz, T., Small, E. & Silberberg, Y. Looking around corners and through thin turbid layers in real time with scattered incoherent light. *Nature Photon.* **6,** 549–553 (2012).
26. Fienup, J. R. Reconstruction of an object from the modulus of its Fourier transform. *Opt. Lett.* **3,** 27–29 (1978).
27. Dainty, J. C. (ed.) *Laser Speckle and Related Phenomena* (Springer, 1984).
28. Abbey, B. *et al.* Lensless imaging using broadband X-ray sources. *Nature Photon.* **5,** 420–424 (2011).
29. Thurman, S. T. & Fienup, J. R. Phase retrieval with signal bias. *J. Opt. Soc. Am. A* **26,** 1008–1014 (2009).
30. Wang, L. V. & Hu, S. Photoacoustic tomography: *in vivo* imaging from organelles to organs. *Science* **335,** 1458–1462 (2012).

Author Contributions All authors take full responsibility for the content of the paper.

Author Information Reprints and permissions information is available at www.nature.com/reprints. The authors declare no competing financial interests. Readers are welcome to comment on the online version of the paper. Correspondence and requests for materials should be addressed to J.B. (j.bertolotti@utwente.nl).